ICAS Paper No. 70-48

SOME EXPERIMENTS ON TWO-STREAM PROPELLING NOZZLES FOR SUPERSONIC AIRCRAFT

by
W. G. E. Lewis, Head of Engine Research Department
and
F. W. Armstrong, Section Leader
National Gas Turbine Establishment
Pyestock Farnborough Hants, U.K.

The Seventh Congress of the International Council of the Aeronautical Sciences

CONSIGLIO NAZIONALE DELLE RICERCHE, ROMA, ITALY / SEPTEMBER 14-18, 1970

Price: 400 Lire

SOME EXPERIMENTS ON TWO-STREAM PROPELLING NOZZLES FOR SUPERSONIC AIRCRAFT

W. G. E. Lewis and F. W. Armstrong
National Gas Turbine Establishment
Pyestock, Farnborough, Hampshire, England

Abstract

The experimental technique developed at NGTE for evaluating the internal performance of supersonic propelling nozzles is outlined. An investigation of a family of axisymmetric, two-stream ejector-type nozzles designed for sustained cruising flight at around Mach 2, is then described.

With the primary nozzle throat diameter and final shroud exit diameter maintained constant, the effects were explored of varying the shroud throat/primary throat area ratio, and the axial spacing between the primary and shroud throats. Each configuration was tested at conditions appropriate to supersonic cruise, over a range of secondary/primary airflow ratio. The results are presented in terms of gross gauge thrust efficiency and secondary airflow acceptance characteristics.

I. Introduction

The achievement of high propelling nozzle performance in supersonic flight is vital to the success of any aircraft designed to cruise supersonically for prolonged periods. For such projects, the payload fraction is small compared with subsonic aircraft, and the ratio of gross to net thrust is high. As a result, the penalty in range/payload performance for a shortfall in nozzle gross thrust efficiency is inevitably severe.

This situation accentuates the need to obtain high quality nozzle performance data from experiments at model scale. Close experimental repeatability and consistency is required for the comparative evaluation of design variations, and a high level of absolute accuracy is essential to permit the reliable prediction of overall project performance. This paper describes the technique developed at NGTE for evaluating the internal performance of propelling nozzles, and presents results for a family of two-stream ejector-type nozzles designed for cruising flight in the region of Mach 2.

II. Parameter definitions

The most important performance parameter for a propelling nozzle is its thrust efficiency. For aircraft project estimates, the relevant internal efficiency is the gross gauge thrust efficiency, η_F, defined as

$$\eta_F = \frac{\text{actual thrust developed for a given applied pressure ratio}}{\text{thrust of an isentropic nozzle passing the same airflow and working over the same applied pressure ratio}} \qquad (1)$$

The applied pressure ratio (APR) is the ratio of the nozzle entry total pressure to the pressure immediately surrounding the nozzle exit, i.e. the 'base' pressure. Due to the flow field around the aircraft, this base pressure may differ from atmospheric static pressure. However, as it is clearly the base pressure which determines the flow conditions within the nozzle, correlation of internal performance must be made in terms of APR. For any particular aircraft project, it then remains to determine the relation between base pressure and atmospheric pressure in flight, by special experiments where an external flow is passed over a model of the appropriate part of the aircraft.

A second thrust efficiency concept, applied in the present context for test rig calibration purposes, is the gross vacuum or absolute thrust efficiency, η_S, defined as,

$$\eta_S = \frac{\text{actual vacuum thrust}}{\text{vacuum thrust of an isentropic nozzle passing the same airflow}} \qquad (2)$$

The vacuum or absolute thrust is the thrust that would be obtained with an APR of infinity, i.e. with a base pressure of zero.

Equations (1) and (2) represent general definitions, in physical terms, of η_F and η_S. These equations can then be particularised according to the type of nozzle under consideration. For the two-stream ejector-type nozzle intended for high efficiency supersonic cruising, the denominator in the efficiency equation will be the sum of the isentropic thrusts of the two streams, assuming full convergent-divergent expansion of each. Thus for this class of nozzle, Equation (1) particularises to,

$$\eta_F = \frac{\text{actual gauge thrust for a given APR}}{W_J V_J^* + W_S V_S^*} \qquad (3)$$

- where W_J and W_S are respectively the primary and secondary flow rates, and V_J^* and V_S^* are the velocities of the primary and secondary streams after isentropic expansion over their respective pressure ratios. APR for a two-stream nozzle is normally quoted in terms of primary stream total pressure to base pressure, the secondary stream having usually a much lower pressure.

Another particular type of nozzle of interest here is the single-stream, purely convergent variety, where the exit and geometric throat planes coincide. A design of this type is used as a standard for rig calibration at NGTE, and for this purpose it becomes convenient to work in terms of a vacuum convergent thrust efficiency, defined as,

$$\eta_{S\ conv} = \frac{\text{actual vacuum thrust}}{\text{vacuum thrust of an isentropic convergent nozzle passing the same airflow}} \quad (4)$$

Now if A_g = nozzle exit geometric area,
P_b = nozzle base pressure,
W = nozzle airflow rate,
T_t = nozzle entry total temperature,
and K = constant, depending on the value of the specific heat ratio, γ

it can be shown that when the nozzle is choked, Equation (4) reduces to

$$\eta_{S\ conv} = \frac{\text{measured gauge thrust} + A_g P_b}{K \times W\sqrt{T_t}} \quad (5)$$

Equation (5) is used, as will be seen later, to obtain a flow calibration for the propelling nozzle test rig.

The final parameter requiring definition here is not an efficiency but a thrust coefficient, found to be of particular value in the analysis of data from two-stream nozzle performance tests. This is the vacuum or absolute specific thrust coefficient, K_{TAI}, defined as,

$$K_{TAI} = \frac{\text{Actual vacuum thrust of two-stream nozzle}}{P_J \cdot A_J^*} \quad (6)$$

- where P_J = total pressure of primary stream at nozzle entry
and A_J^* = isentropic throat area of primary flow

The significance and method of using K_{TAI} will be discussed later, in Section VI.

III. The test rig

Tests at NGTE on supersonic propelling nozzles are carried out using the thrust measuring rig shown schematically in Figure 1. The model nozzle under test is mounted on a sting which is floated horizontally in two air bearings. Dried air is supplied radially to the sting from a collector box, so that its horizontal component of momentum at entry to the floating system is zero. For testing two-stream nozzles there is provision for dividing the sting airflow into two separately metered streams. For testing at the high nozzle expansion ratios appropriate to flight at around Mach 2, the nozzle under test is enclosed by a depression box which leads to an exhaust diffuser. Axial movement of the sting system under the thrust of the nozzle is resisted by a hydraulic thrust measuring capsule. The size of the rig is such that a convenient throat diameter for the primary nozzle is about 3 inches (7.5 cm). With typical air supply conditions of 4 atmospheres absolute pressure, and a temperature of about 25°C, this model size gives a Reynolds Number, referred to nozzle throat conditions, of about 4×10^6. This is equivalent to the full-scale value for an aircraft having propelling nozzles of about 35 inches (89 cm) throat diameter, cruising at Mach 2 around 55,000 ft (17 km).

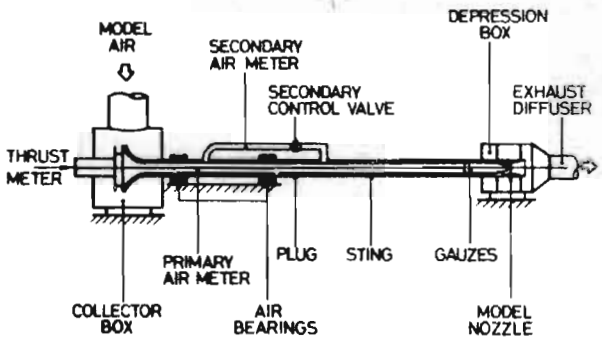

FIG.1 NOZZLE TEST RIG

IV. Rig accuracy and calibration

The determination of gauge thrust efficiency, η_F, involves the direct measurement of actual nozzle thrust, and the derivation from other test readings of the corresponding isentropic thrust. The achievement of good accuracy for η_F therefore requires that a number of quantities be determined to high standards of accuracy. Notes on the problems and procedures involved are given below.

Actual gauge thrust

In addition to the obvious need for an accurate force measuring device, the achievement of an accurate nozzle thrust value demands careful rig design, followed up by painstaking development aimed at minimising extraneous forces. The mounting of the sting assembly in air bearings is an important design feature. Special calibration tests to obtain corrections for the small forces arising from air leakage at the labyrinth seals between collector box and sting, and depression box and sting, were carried out in the early rig development phase. As a part of this activity, it was also necessary to pay attention to the careful setting up of these seals.

Isentropic gauge thrust

Referring back to the definition expressed by Equation (3), the isentropic gauge thrust for the two-stream nozzles under consideration here is,

$$F_{G\ is} = W_J V_J^* + W_S V_S^* \quad (7)$$

- where V_J^* and V_S^* relate to full expansion over the APR's of the primary and secondary streams respectively. Now considering the problem of obtaining an accurate value for $F_{G\ is}$, the first point to note is that W_S and V_S^* are small by comparison with W_J and V_J^* respectively, so that the secondary stream contributes only a few percent of the total thrust in a typical case. Small percentage errors in evaluating the secondary isentropic thrust will therefore be insignificant in their effect on $F_{G\ is}$, and adequate accuracy is obtained by measuring the secondary flow rate with a standard orifice plate and the secondary total pressure by pitot tubes mounted in the annulus approaching nozzle entry.

The primary stream, however, demands much closer attention. It is useful at this stage to rewrite the primary isentropic thrust as

$$W_J V_{J*} = W_J\sqrt{T_t} \cdot \frac{V_{J*}}{\sqrt{T_t}} \qquad (8)$$

In Equation (8) the value of $\frac{V_{J*}}{\sqrt{T_t}}$ is that value of $\frac{V}{\sqrt{T_t}}$ in the standard airflow tables which corresponds with a value of $\frac{P_t}{P_s}$ equal to the primary stream APR. Now it so happens that as flow Mach number increases, the curve of $\frac{V}{\sqrt{T_t}}$ versus $\frac{P_t}{P_s}$ decreases in slope - i.e. $\frac{V}{\sqrt{T_t}}$ becomes less sensitive to an error in $\frac{P_t}{P_s}$. For an APR value characteristic of cruise in the region of Mach 2, say 12 to 16, this effect has progressed to the degree that a 1 per cent error in $\frac{P_t}{P_s}$ would cause only about $\frac{1}{10}$ per cent error in $\frac{V}{\sqrt{T_t}}$. At the same time, by inspection of Equation (8) it is clear that a 1 per cent error in the product $W_J\sqrt{T_t}$ will always cause a 1 per cent error in the primary isentropic thrust. Thus the emphasis must be placed on getting an accurate value for $W_J\sqrt{T_t}$, with the absolute accuracy of the nozzle entry total pressure being of much lesser importance. In fact, the sensitivity of η_F to $W_J\sqrt{T_t}$ is about the same as its sensitivity to nozzle actual thrust, for cases where the secondary flow and thrust contribution are relatively small.

Now it has already been mentioned, under 'Parameter definitions', that for flow calibration work at NGTE a particular design of convergent nozzle is used as a standard. Considerable attention has been paid to establishing within close limits the thrust efficiency of this design, using accurate thrust measurements on a 'reference' thrust rig in conjunction with theoretical considerations which provide a close estimate of the nozzle discharge coefficient. An outline of this background work is given in Reference 1; its application in calibrating the thrust rig shown in Figure 1 is described below.

The approach is to make use of Equation (5), derived from the definition of $\eta_{S\ conv}$. A minor rearrangement of Equation (5) yields,

$$W\sqrt{T_t} = \frac{\text{measured gauge thrust} + A_g P_b}{K\,\eta_{S\ conv}} \qquad (9)$$

The numerator of this equation is the actual vacuum thrust, which is invariant with APR as long as the nozzle remains choked. Hence if the rig to be calibrated is run in the single-stream mode with a standard convergent nozzle fitted, a value for $W\sqrt{T_t}$ can be obtained from thrust and back pressure measurements, combined with the known $\eta_{S\ conv}$ for the standard nozzle. Now if reference total and static pressures are measured simultaneously at a convenient station in the approach pipe (plane 1 in Figure 2), then by successively running the rig with a range of standard convergent nozzles of differing throat area Ag, a rig flow calibration curve of the form shown in Figure 2 can be obtained. For subsequent tests of other nozzles on the rig, this calibration curve will yield a value of $\frac{W\sqrt{T_t}}{P_{t_1}}$ from the reference station measurement of $\frac{P_t}{P_s}$.

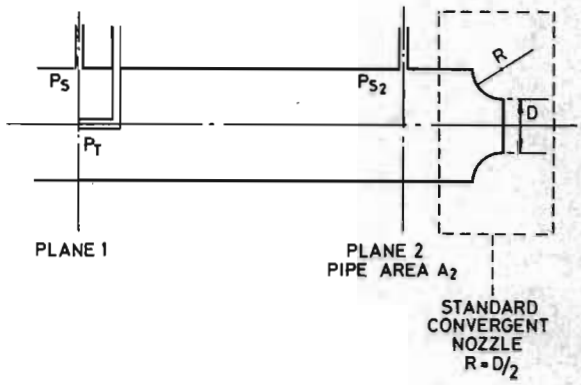

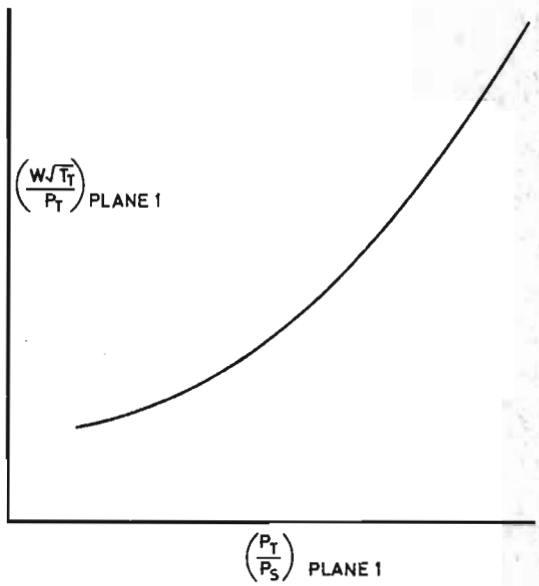

FIG.2 RIG CALIBRATION

Another essential measurement in the calibration process is the static pressure at the plane regarded as defining 'nozzle entry'. Using this pressure in conjunction with the pipe area A_2 and the corresponding value of $W\sqrt{T_t}$ found by applying Equation (9), the compressible airflow function $\frac{W\sqrt{T_t}}{A_2 P_{s2}}$ can be obtained. From this, the function $\frac{P_{t_2}}{P_{s2}}$ follows, thus giving a 'mass flow derived' value for total pressure at nozzle entry, P_{t_2}. Because of flow profile effects, this value for P_{t_2} will not in general be quite the same as the mass-weighted mean total pressure. However, we have seen from a preceding argument that the sensitivity of η_p to AFR is much less than to $W\sqrt{T_t}$, and therefore the method outlined above for obtaining P_{t_2}, and hence AFR, is of sufficient accuracy.

So far no mention has been made of 'real air' effects on either the rig calibrations or on test nozzle performance. Regarding these, it may first be noted that the NGTE 'reference' rig described in Reference 1 operates with atmospheric inlet conditions for both pressure and temperature. In this situation, the error incurred by assuming $\gamma = 1.4$ in calculating $\eta_{S\ conv}$ for the standard calibration nozzle is less than 0.04 per cent. This is well within the experimental accuracy of that rig, and has therefore been ignored.

In the rig illustrated in Figure 1, the maximum inlet pressure is about 4 atmospheres. At this pressure level, and with a typical nozzle entry temperature of 25°C, the specific vacuum thrust, $\frac{X_{GA\ real}}{W\ real}$, is approximately 0.1 per cent less than with 'classic air', i.e. where $\gamma = 1.4$. In other words, if the test rig was measuring the 'real' airflow correctly an error of this order of magnitude could arise in the derived thrust efficiency using an isentropic thrust based on 'classic air'. However, the calibration technique adopted is such that in fact there is derived from it a corrected value of $W\sqrt{T_t}$ such that the absolute level of thrust efficiency is independent of pressure level, and always equal to the value given by the reference thrust rig with its negligibly small error.

Turning now to the overall standards of accuracy achieved for the test rig, the only categorical statement that can be made is that derived η_p results show repeatability within ±0.15 per cent, and in many instances within ±0.10 per cent. These ranges reflect the small random scatter of the experimental measurements and successive calibrations. It is naturally much more difficult to make an estimate of absolute accuracy; this depends upon systematic errors which, by their very nature, can be highly elusive. What can be said, however, is that the rig has been subjected to a serious and continuing development programme with the object of establishing a high degree of confidence in the absolute level of the results produced. While it is always possible that some unsuspected systematic error may exist in an experimental apparatus, the likelihood of this can be minimised by careful investigation of possible sources of such errors. This is the course we have tried to pursue.

V. The test nozzles and instrumentation

A sketch of the basic geometry and the dimensions defining a family of two-stream nozzles investigated are shown in Figure 3.

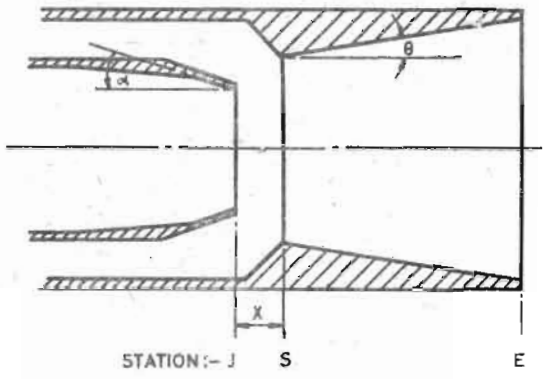

BASIC NOZZLE PARAMETERS

A_J = 7·277 SQ. INS (46·9 SQ. CMS.)

$\frac{A_E}{A_J}$ = 2·75

θ = 9°

α = 16°

$\frac{A_S}{A_J}$	1·4	1·5	1·6	1·7	1·8
$\frac{X}{D_J}$	—	·06	·06	—	—
	·086	·097	—	—	—
	—	·14	·14	·14	·14
	·166	—	·155	—	—
	·22	·22	·22	·22	·24
	—	—	·27	—	—
	—	·3	·3	·3	—
	·45	·45	·45	·45	·46

FIG.3 EJECTOR NOZZLE DIMENSIONS

These nozzles were designed for use as part of an integrated powerplant suitable for cruise at about Mach 2, where the air bled from the intake would be

passed around the engine carcase and jet pipe, finally forming the secondary stream of the ejector-type nozzle. Having originated as an intake boundary layer bleed, and suffered further loss of total pressure on its way past the engine, the nozzle secondary stream in such an installation must be at a relatively low pressure compared with the primary stream coming from the engine jet pipe. To obtain ample coverage of matching conditions likely to be of practical interest, the model nozzle configurations were planned to obtain a range of secondary to primary total pressure, $\frac{P_s}{P_J}$, of about 0.15 to 0.3, and a range of non-dimensional flow ratio, $\mu \left(= \frac{W_S\sqrt{T_S}}{W_J\sqrt{T_J}} \right)$, about 0.02 to 0.12.

The nozzle instrumentation comprised at least two static pressure tappings at opposite extremes of a diameter across the shroud base, four static tappings spaced around the circumference of the primary nozzle 'jet pipe' in a plane (plane 2 of Figure 2) approximately two primary nozzle diameters upstream of the primary nozzle exit plane, and a pair of pitot tubes diametrically opposed in the secondary flow annulus coplanar with the four jet pipe statics.

VI. Experimental and analytical procedures

The nozzles were tested over a range of APR extending from about 12 to 18 - i.e. conditions appropriate to supersonic cruise. For each configuration a range of non-dimensional flow ratio μ, of about 0.02 to 0.12 was obtained by variation of the secondary control valve shown in Figure 1. This simply changed the value of $\frac{P_s}{P_J}$, allowing the nozzle to rematch at a different μ. It should be noted that both primary and secondary streams have the same total temperature in this rig; therefore although the results are correctly plotted in terms of the non-dimensional flow ratio μ, this was numerically given by the direct flow ratio $\frac{W_S}{W_J}$ in the tests.

At each nozzle operating point the following measurements were taken:-

(a) primary airmeter, total and static pressures (plane 1 of Figure 2)

(b) secondary airmeter pressures

(c) secondary nozzle entry total pressure (plane 2 of Figure 2)

(d) primary nozzle entry static pressure (plane 2 of Figure 2)

(e) shroud base pressure

(f) depression box static pressure

(g) barometric pressure

(h) thrust capsule pressure

Concerning the determination of nozzle performance from these measurements, making use of the rig calibration data as previously outlined, most of the procedures are essentially self-evident and will not be set out here. One procedure which is not in this class, however, is of sufficient importance to merit a brief description. This is the calculation to obtain the gross gauge thrust efficiency, η_F. One way of obtaining values for η_F is to use directly the measured gauge thrust, and other test readings, for each nozzle operating point in turn. With this method each calculated figure for η_F is subject to the scatter inherent in the readings at any individual test point, and plots of η_F derived by this means, against operating parameters such as μ, exhibit this scatter. It then remains to fit the best curve through the η_F points.

The alternative method of handling experimental data is to smooth out the scatter at some intermediate stage. This is preferable if the final stages in the derivation of the desired quantity tend to magnify scatter by virtue of the algebraic operations involved. In the present context, experience has shown the following procedure to be an effective way of minimising the influence of scatter on the derived η_F characteristics.

The first step is to express the test data from individual operating points in terms of the absolute specific thrust coefficient, K_{TAI}, defined in Equation (6).

Now K_{TAI} is a constant independent of APR at any particular point on the ejector characteristic relating $\frac{P_s}{P_J}$ to μ - <u>provided</u> that the APR is sufficiently high for the nozzle to be running full. Therefore all the values of K_{TAI} calculated directly from all the experimental points for all pressure ratios with any particular nozzle running full, will fall about a single curve relating K_{TAI} to μ. Hence, if at any given value of μ, the thrust efficiency at a given APR is derived from K_{TAI}, this itself being read from the unique curve just defined, the resultant efficiency value will reflect an averaging of all the test data at all pressure ratios. It is a simple matter to derive in this way curves of η_F versus μ for a series of chosen APR's, all from the same 'smoothed' K_{TAI} curve. Figure 4 shows a typical set of results, for one nozzle configuration, treated in this way. The individual test points are shown on the K_{TAI} versus μ, and $\frac{P_s}{P_J}$ versus μ characteristics, while the least squares curve through the K_{TAI} points yields the smooth curves shown for η_F versus μ for APR's of 12, 14, 16 and 18.

Special tests conducted simultaneously with those reported here showed, with the aid of extensive pressure plotting in the divergent shroud,

that APR's of nearly 12 were needed to make the nozzles run full. Therefore to obviate any errors in the K_{TAI} analysis only results for measured APR's of 12 or more were used in the derivation of the η_F curves.

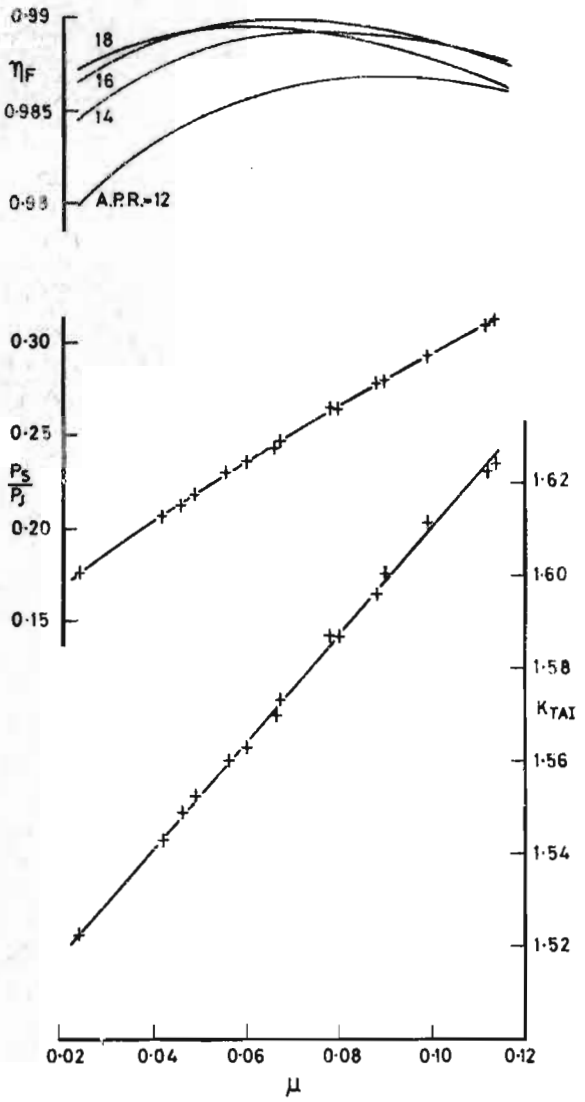

FIG.4 TYPICAL RESULTS

$\frac{A_S}{A_J}$ = 1·5, $\frac{X}{D_J}$ = 0·22

VII. Results and discussion

Due to the number of configurations tested, and the operating variables for a two-stream nozzle, a complete presentation of the results of this investigation is not possible in the space available here. An attempt will therefore be made to outline the most significant features of the results, paying particular attention to the implications for the choice of nozzle design for the choice of nozzle design for an aircraft project.

Some simplification can be obtained by concentrating mainly on a single, typical, APR value. This is also appropriate because APR is a quantity that would be independently specified during aircraft project studies, from considerations of intake and engine performance, and an estimated likely base pressure/atmospheric pressure relationship. For cruise at about Mach 2, a typical APR value could be 14, and this has been chosen for the comparisons made here. It can be noted though, before proceeding further, that variations about this value of 14 will not greatly alter the comparative picture. For example, the main effect of raising the APR to 16 would be to lift the general level of thrust efficiency very slightly, and reducing APR to 12 would have an opposite, and somewhat stronger, effect. Figure 4 gives a typical indication.

Another parameter likely to be confined within fairly close limits as a result of overall aircraft powerplant considerations is the non-dimensional secondary flow ratio, μ. As this determines the required $\frac{P_S}{P_J}$ for a given configuration, as well as exerting a significant influence on thrust efficiency, results are presented here for two values in the range of likely practical interest, namely μ = 0.06 and 0.04.

Figure 5 therefore shows η_F and $\frac{P_S}{P_J}$ characteristics, as functions of the geometric parameters $\frac{A_S}{A_J}$ and $\frac{X}{D_J}$, for operation at μ = 0.06, APR = 14, while Figure 6 is a similar presentation for μ = 0.04 and the same APR. The first point to be noted from these Figures is that for most configurations tested, the gauge thrust efficiency lies between 0.98 and 0.99. The difference between these two levels is of course significant in terms of supersonic range/payload, for with a typical gross to net thrust ratio of about $2\frac{1}{2}$, a 1 per cent difference in η_F is equivalent to $2\frac{1}{2}$ per cent on installed net thrust and specific fuel consumption.

At constant APR and μ, nozzles having a given $\frac{A_S}{A_J}$ show a maximum thrust efficiency at a particular axial spacing, $\frac{X}{D_J}$, between the primary exit and the shroud throat. This optimum axial spacing increases as $\frac{A_S}{A_J}$ is increased, so that for the higher $\frac{A_S}{A_J}$ configurations the maximum η_F occurs at, or just beyond, the highest tested $\frac{X}{D_J}$ of 0.45. The level of this thrust efficiency maximum falls progressively as $\frac{A_S}{A_J}$ is increased, an important effect also found in the studies of Reference 2. Considering this trend in reverse, however, it is likely that extending the tests to include values of $\frac{A_S}{A_J}$ lower than 1.4 would show

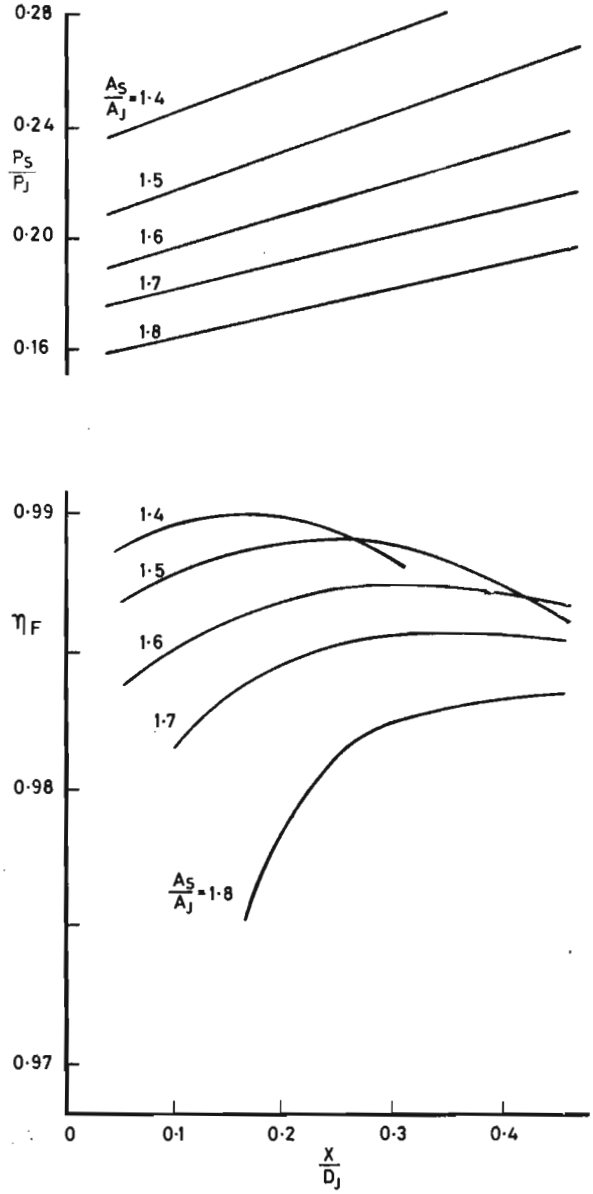

FIG.5 NOZZLE PERFORMANCE CHARACTERISTICS FOR A.P.R.= 14 AND μ = 0·06

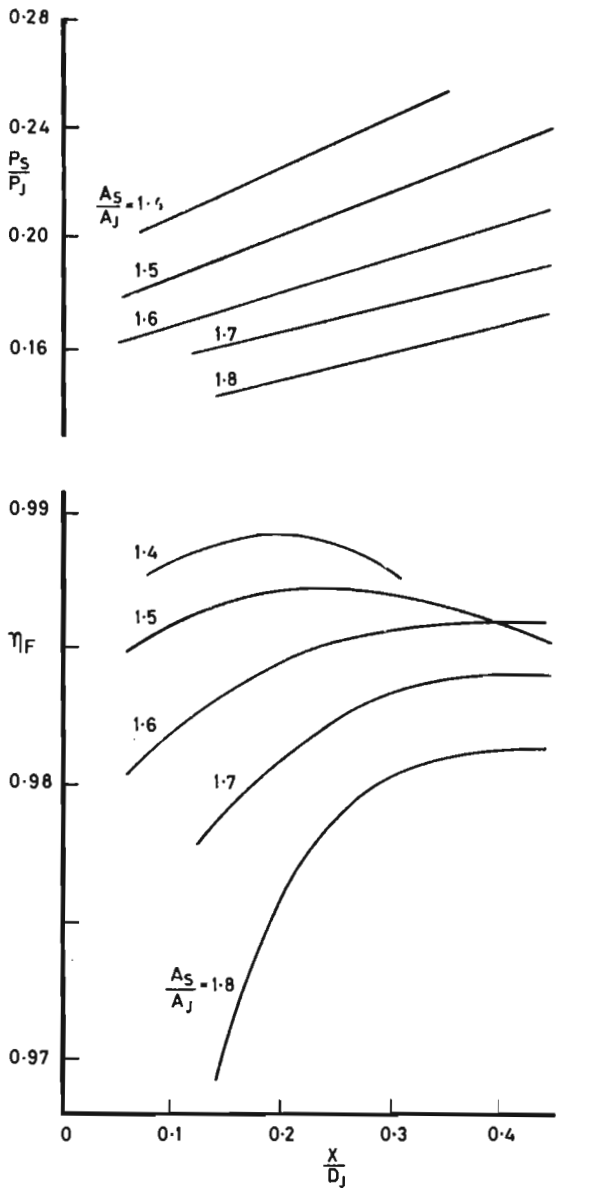

FIG.6 NOZZLE PERFORMANCE CHARACTERISTICS FOR A.P.R.= 14 AND μ = 0·04

only little, if any, further increase in the maximum η_F achievable. At μ = 0.06, the curves of Figure 5 suggest that an $\frac{A_S}{A_J}$ of 1.3 might well give a maximum η_F level equal to, or even below, that for $\frac{A_S}{A_J}$ = 1.4, although for μ = 0.04 (Figure 6) there would probably be some small gain with $\frac{A_S}{A_J}$ = 1.3. In this latter case, the use of $\frac{A_S}{A_J}$ = 1.3 might result in the raising of the maximum η_F to about 0.99 - i.e., a similar level to the maximum for $\frac{A_S}{A_J}$ = 1.4 at μ = 0.06.

The physical reasons for the shape of the thrust efficiency characteristics are obviously

associated with the flow conditions within the nozzle. These conditions are not known in detail but the diagram of Figure 7 has been put forward (Reference 3) as a representation of the possible general situation in a nozzle of this type. It is postulated that the initial expansion of the primary flow, downstream of the primary nozzle exit plane, is influenced to a varying degree by the surrounding secondary flow. If the geometric parameters $\frac{A_S}{A_J}$ and $\frac{X}{D_J}$ are not well matched to the nozzle operating variables μ and $\frac{P_s}{P_J}$, the primary expansion may be relatively 'uncontrolled' so that the boundary of the now supersonic primary stream then suffers an abrupt change of shape when it comes within the influence of the divergent wall of the shroud. The strength of the resulting shock is clearly dependent on the prevailing conditions. Related factors such as the shroud wall boundary layer state and the rate of mixing between primary and secondary flows will also play a part in determining the wall pressure distribution and friction drag, the overall interaction being doubtless of a complex nature. The general evidence from the family of nozzles tested here, however, suggests strongly that for the higher values of $\frac{A_S}{A_J}$, the shroud throat and divergent walls are simply too far away from the nozzle centre-line for the primary stream expansion to be controlled in a proper way, even when a high value of secondary flow ratio is used.

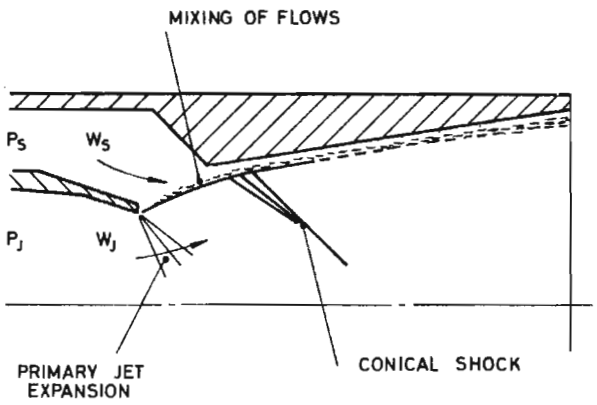

FIG.7 POSSIBLE NOZZLE FLOW CONDITIONS

The effect of the geometrical parameters of the nozzles tested upon their secondary flow acceptance characteristics, $\left(\frac{P_s}{P_J} \text{ versus } \mu\right)$ is a matter of considerable practical significance. For a given $\frac{A_S}{A_J}$, the value of $\frac{P_s}{P_J}$ required for operation of the nozzle at a given μ increases with the axial spacing $\frac{X}{D_J}$, while reduction of $\frac{A_S}{A_J}$ at a constant axial spacing has a similar effect. The secondary flow acceptance characteristic does not depend on the value of APR, provided that the secondary flow field is 'frozen' by choking at some point in the stream - a condition confirmed by supplementary experiments as existing over the range of results reported here.

The salient features of the results having been described, it is of interest to consider the implications of aiming for the highest possible efficiency level. We have seen that working within the general scantlings of this family of nozzles, a gross gauge thrust efficiency of about 0.99 is attainable at an APR of 14 if appropriate values of the internal geometric variables $\frac{A_S}{A_J}$ and $\frac{X}{D_J}$ are selected. If the design is intended to operate at a μ of 0.06, an $\frac{A_S}{A_J}$ of 1.4 needs to be combined with an $\frac{X}{D_J}$ of about 0.15 - although the η_F curve is very flat in the $\frac{X}{D_J}$ range 0.1 to 0.2. For operation at $\mu = 0.04$, the optimum combination would be $\frac{X}{D_J}$ about 0.2, and $\frac{A_S}{A_J}$ about 1.3. Having determined the optimum geometry from the thrust efficiency characteristics, the secondary nozzle acceptance data must be used to decide the $\frac{P_s}{P_J}$ required to enable the nozzle to run at the chosen condition. For $\mu = 0.06$ operation of a nozzle with $\frac{A_S}{A_J} = 1.4$ and $\frac{X}{D_J} = 0.15$, the required $\frac{P_s}{P_J}$ (from Figure 5) is roughly 0.25. It so happens that a similar value will be required for $\mu = 0.04$, $\frac{A_S}{A_J} = 1.3$, $\frac{X}{D_J} = 0.2$ (extrapolating the data of Figure 6).

Now a $\frac{P_s}{P_J}$ level of 0.25 lies towards the upper end of the range recorded for this parameter in the series of designs tested. There is in fact a correlation, though not a unique one, between $\frac{P_s}{P_J}$ and η_F for this family of nozzles when operated at constant APR and μ. For example, if the data of Figure 5 is replotted in terms of η_F versus $\frac{P_s}{P_J}$ for the various $\frac{A_S}{A_J}$ and $\frac{X}{D_J}$ values covered by the tests, this broad relationship emerges quite clearly - see Figure 8. In general, configurations which can run at this μ value with lower values of $\frac{P_s}{P_J}$, will have lower efficiencies, while higher $\frac{P_s}{P_J}$'s are needed for configurations offering higher efficiencies.

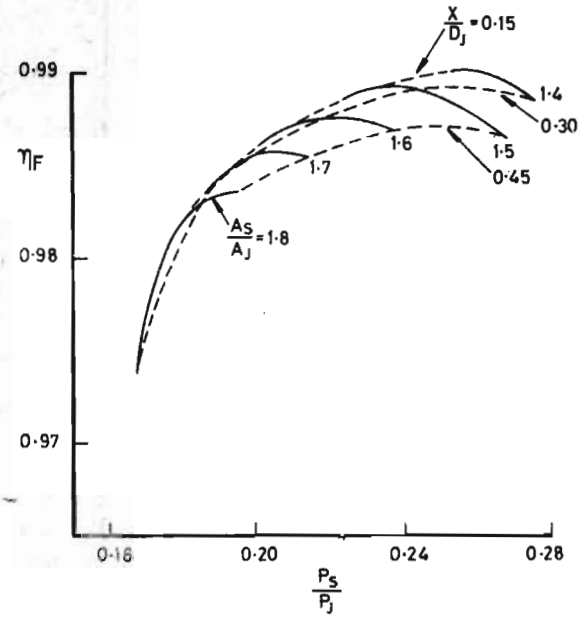

FIG.8 THE INFLUENCE OF $\frac{P_S}{P_J}$ ON EFFICIENCY

A.P.R.=14, μ=0·06

This brings out the fact that if the overall powerplant design is such as to limit unduly the value of $\frac{P_s}{P_J}$ - for example, by excessively high pressure losses as the secondary air flows past the engine - then it might be impossible to exploit properly the efficiency potential of a given class of propelling nozzle. For example, if with the operating conditions of Figure 8 (APR = 14, μ= 0.06) the value of $\frac{P_s}{P_J}$ cannot be raised above, say 0.20, then the highest achievable nozzle thrust efficiency, assuming complete freedom in the choice of $\frac{A_S}{A_J}$ and $\frac{X}{D_J}$, would be about 0.986. It should be noted that when nozzle efficiency suffers as shown above, the adverse performance effect of a low P_s, for a constant P_J, is a double one. For even with nozzle efficiency constant, the reduction in secondary expansion ratio would cause a loss of thrust.

It can be seen from the foregoing discussion that in any particular aircraft application, the efficiency of a nozzle of the class investigated here could be restricted to a level lower than its potential maximum by either of two quite separate types of limitation. First, considerations of structural or mechanical design in the nozzle region could prevent an optimum choice of the internal geometric parameters $\frac{A_S}{A_J}$ and $\frac{X}{D_J}$, and second, $\frac{P_s}{P_J}$ available at the nozzle could be too low. Finally, it must be borne in mind that it is the overall performance that matters for an aircraft project. A design compromise which reduces the internal cruise thrust performance might be justified if it produces savings in weight or external drag, or improvements in performance at an important off-design condition.

VIII. Conclusions

1. With careful rig design and development, it is possible to determine the performance of propelling nozzles, at model scale, to the high standards of consistency and accuracy that are needed for the evaluation of aircraft projects involving prolonged cruise at supersonic speeds.

2. For the class of two-stream propelling nozzles investigated here, designed for cruise at Mach 2 or thereabouts, an internal gross gauge thrust efficiency of about 0.99 is available provided that:-

   (a) other design considerations do not prevent optimisation of the internal geometry of the nozzle,

   (b) the ratio of the secondary to primary pressures at nozzle entry is sufficiently high.

It should be noted that this efficiency figure of 0.99 is the level recorded for a model with a clean internal profile, running with cold airstreams but with a Reynolds Number in the region of a full-scale aircraft value.

Acknowledgement

The work reported here, covering the design and development of a high accuracy rig, followed by the investigation of numerous propelling nozzle configurations, has involved the efforts, over a period of time, of a number of NGTE personnel. Particular acknowledgements are due to M. C. Neale, D. E. Glenny, P. G. Street, J. S. Drabble and J. P. Edwards.

References

1. Propelling nozzle research, W. G. E. Lewis, J.Roy.Aero.Soc., Vol. 68, No. 647, November 1964.

2. Inlet duct-engine exhaust nozzle airflow matching for the supersonic transport, J. B. Taylor (G.E.C. Cincinnati), AIAA Paper No. 67-574, October 1967

3. Theoretical study of an aerodynamic supersonic nozzle, M. J. Hardy, Agardograph 103, October 1965